IEEE Access
Multidisciplinary ⋮ Rapid Review ⋮ Open Access Journal

Received 24 January 2023, accepted 20 March 2023, date of publication 29 March 2023, date of current version 3 April 2023.

Digital Object Identifier 10.1109/ACCESS.2023.3262986

RESEARCH ARTICLE

Hybrid Condition Monitoring for Power Converters: Learning-Based Methods With Statistical Guarantees

NIKOLA MARKOVIC[1], (Graduate Student Member, IEEE), THOMAS STOETZEL[2], (Student Member, IEEE), VOLKER STAUDT[2], (Senior Member, IEEE), AND DOROTHEA KOLOSSA[1], (Senior Member, IEEE)

[1]Institute of Energy and Automation Technology, Technische Universität Berlin, 10587 Berlin, Germany
[2]Department of Power Systems Technology and Power Mechatronics, Ruhr University Bochum, 44801 Bochum, Germany

Corresponding author: Nikola Markovic (nikola.markovic@tu-berlin.de)

This work was supported by the German Federal Ministry for Economic Affairs and Climate Action under Grant 03ET7554B, Grant KK5110703LF1, and Grant KK5479701LF2.

ABSTRACT In this paper, a new learning-based method is proposed for the early detection of changes of parameters in power converters. It circumvents the pertinent shortcomings of previous model-based methods, such as their need for acquiring switching signals, dependence on the control method, or the need for isolating a part of the system during monitoring and thus interfering with the system performance or its start-up time. Additionally, a downside of the learning-based approaches, which is that their performance depends on the quality of the measurements, is addressed through constructing hybrid models that combine the benefits of both lines of development. Our approaches are evaluated with several types of features based on wavelet decomposition and empirical mode decomposition. Using these, an ANN-based classifier is trained for fault detection. For achieving the final decision on the presence or absence of a fault state, we propose the use of sequential hypothesis testing. This hybrid approach yields a much higher reliability than instantaneous ANN-based classification, while allowing for a statistically sound cross-temporal information integration and providing a controllable error bound for the probability of misclassifications. The proposed method was evaluated on two data-sets recorded from a buck converter and an arm of a modular multilevel converter. The results show that, for both systems, the proposed method is capable of reliably recognizing changes of the system parameters. The potential for practical applications is shown through an implementation on a low-power-consumption microcontroller.

INDEX TERMS Fault diagnosis, power converters, DC/DC Converter, MMC, machine learning, signal processing, hybrid models.

I. INTRODUCTION

condition monitoring of power converters in energy systems is of great importance, considering the wide range of applications in which they play a critical role, and their long operational time. While there are many different power converter topologies, these broadly share the same principles of operation via active and passive elements. Hence, very similar condition monitoring methods can, with some modifications, be applied for different power converters.

The specific condition monitoring technique proposed in this paper is applied to two different power converter topologies. The first is a buck converter, a widely employed DC-DC power converter [1]. The second system is an arm of a of modular multilevel converter (MMC). These converters have gained great interest in academia as well as industry shortly after they were initially proposed [2], due to their modular design, their scalability, the good quality of the output

The associate editor coordinating the review of this manuscript and approving it for publication was Ahmed Aboushady.

voltage, low switching losses, and the fact that redundancy can be easily achieved [3].

A. RELATED WORK

The reliability as well as fault detection & isolation (FDI) of power converters have recently attracted significant research attention. The most fragile components in these systems are the semiconductor devices [4] and passive elements, primarily capacitors, but also inductors and resistors [5], [6]. Faults of semiconductor devices are categorized into short- and open-circuit faults. Short-circuit (SC) faults require a very fast response, which is why they are usually handled at the hardware level [7], [8]. Open-circuit (OC) faults, in contrast, do not always have an immediate impact on the performance of the system, especially in large systems. Degradations of the passive elements are usually very slow and their reliable detection is therefore a challenging albeit important task, as they can cause violation of the output voltage and power specifications. While most prior research is focused on semiconductor faults, this work is concerned with applying data-based methods for early detection of such degradations of passive elements.

1) PARAMETER CHANGES

The methods for FDI in DC-DC converters can be classified as hardware-, model- or data-based [9]. Since hardware-based approaches are not being used for detecting parameter degradations, they are omitted from this discussion. *Model-based* approaches are the most common, with great emphasis being placed on observers. For linear systems, a Luenberger observer is often applied, e.g. in [10], where a bank of two such observers are used to monitor parameter changes. In [11], a general switched linear state estimator for a wide range of power converters is presented for FDI of parameter changes and OC faults as well as sensor faults. An adaptive observer for estimation of capacitance and inductance of a Buck converter is proposed in [12].

Although model-based methods for fault diagnosis are highly developed, they are not always easily applicable to complex power electronic systems. The main reason is their dependence on a precise mathematical system model, which is not easy to derive for large-scale power systems, not least because of the parameter uncertainty that is significant in these types of systems.

For these reasons, *learning-based* (or data-driven) methods, in which the inference about the current state of the system relies only on the available measurements, have been proposed for DC-DC converters. As one recent, notable example, [13] describes a fault detection approach that is independent of the converter structure. This is achieved by monitoring statistical properties of the output signal and measuring their deviation from the previously learned range of normal values. This allows for successful detection, but not isolation of the faults. The authors in [14] also propose a machine-learning method for detecting large parameter changes, utilizing wavelet features and training a classifier based on a deep-belief network for the fault recognition. Another machine-learning approach for larger parameter changes was proposed and applied to a superbuck converter in [15]. Statistical characteristics of the output voltage signal are used as features after a dimensionality reduction and a special type of artificial neural network (ANN)—the *extreme learning machine*—is tasked with the classification of the fault types. In [16], a technique is presented for reliable isolation of parameter changes in power converters. The approach applies wavelet-based features and a simple ANN classier, and its performance is shown on a buck converter connected to a local distribution grid.

Research concerning FDI for the MMC has predominantly focused on semiconductor faults [17]. This has, however, been changing in recent years, with an increasing number of papers being published on detecting failures of the capacitors in the submodules (SMs) of the converter. As in the case of the DC-DC converters, the common approach is to use relations derived from the physical model of the converter to monitor the SM capacitance. In [18], a method is proposed, which uses a simple relation between SM voltage and capacitor current. The capacitor impedance is computed by dividing the root-mean-square values of the two signals' second-harmonic-order components. One drawback of this method is that it cannot be used if circulating current suppression control is applied. The same relation between SM voltage and capacitor current was used in [19], where the error of the capacitance estimation was minimized by recursive least squares (RLS) estimation. Another strategy for a robust estimation is proposed in [20], by employing a Kalman filter. The method proposed in [21] also uses RLS for capacitance estimation, based on modeling the relation between the capacitance and SM voltage change during the fundamental period, when the nearest level modulation control is used. In [22], the authors achieve good capacitance estimation accuracy by using the fundamental frequency component of the capacitor voltage and current.

Another group of recent methods relies on the change in the switching frequencies of the SM semiconductors caused by capacitor deterioration. For example, in [23], the authors model this relation through a polynomial fit, while the authors in [24] propose training an ANN. Similarly, [25] uses the sum of the switching signals in a SM as the indicator for capacitance change. Alternatively, capacitance monitoring is implemented by explicitly monitoring the charging time of the capacitor. The strategy in these approaches [26], [27], is to first isolate each SM and compare the charging time with a reference SM. A downside of this type of approach is that it can take several hours to conduct monitoring for a large MMC.

A data-driven method for detecting capacitance changes in MMCs is proposed in [28]. There, the SM voltage and the arm current signals are used to train a one-class-classifier for detecting changes in capacitance, and T^2 statistics are used to improve the reliability of the system.

2) OC AND SC FAULTS

The majority of the earlier data-driven methods for FDI in power converters were applied to detect OC and SC faults. One interesting example of such a method is presented in [29]. Here, combinational or fuzzy logic is applied for inference based on statistical features, which are extracted from the recorded signals signals. In the method described in [30], principal component analysis (PCA) is applied to monitor Hotelling's T^2 and Q statistics in order to detect the occurrences of OC faults. In [31], a quartile analysis is applied to the capacitor voltages in one arm to detect and isolate OC faults.

A general drawback of these data-driven techniques for condition monitoring is that their performance highly depends on the quality of the measurements and that data recorded at different operation modes of the system is needed to achieve robust performance in practical applications. In recent years, more work was done to overcome these difficulties by applying advanced machine and deep learning methods in combination with different features to train robust classifiers. Bayesian networks in combination with fast Fourier transform (FFT)-based features are successfully applied for detecting and isolating single and double OC faults in a power inverter in [32]. Recently, convolutional neural networks (CNNs) have also shown good results in isolating OC faults by using the wavelet transform to extract features from the measured arm and submodule signals [33]. [34] Reference showed how phase-current signals can be used with CNNs for FDI of single OC faults in a three-phase inverter. A very robust classifier based on a 1-dimensional CNN is designed in [35], using sub-module output voltages and circulating current as the inputs to the network.

From these recent works, it can be seen that data-driven methods are showing promising results for the detection and isolation of semiconductor faults in power electronics. For the problem of parameter change detection, however, data-based approaches are still scarce. However, the advantages of data-driven methods and their performance in power electronics applications so far provides a strong motivation for their application in detecting changes of parameters as well, which is therefore the focus of this work.

B. CONTRIBUTIONS

This paper proposes a novel, learning-based condition monitoring technique for power converters. It relies on signals recorded from the converter to recognize any significant changes of the system parameters. The features used for this purpose are based on signal processing techniques, such as wavelet decomposition and empirical mode decomposition (EMD), which are shown to provide highly informative indicators of the current state of the system. This allows training a relatively simple classifier for system faults, based on deep neural networks, which offers high performance on its own. However, despite the good performance of this direct fault classification, the possibility of false alarms cannot be eliminated with sufficient confidence. For this reason, in order to achieve maximal reliability and validity of the fault detection, we suggest a novel mechanism for integrating instantaneous classifier decisions across time in a statistically sound decision process. This also enables us to provide error bounds on the mis-classification probability of the system, which is valuable in choosing system parameters—specifically related to the speed of decision making—in a task-driven, explainable and systematic way.

The method is evaluated on different power converters, with the use case of detecting changes of capacitance and inductance. We show that the proposed method achieves reliable multi-class classification for all considered types of faults, even during changes of the operating point. Also, the robustness of the approach is evaluated by training the classifier to recognize small parameter changes and then testing on data recorded when the parameter changes are larger.

We further show the applicability of the proposed method to low-resource settings by implementing it on a low-power-consumption microcontroller.

Hence, the contributions of this paper can be summarized as follows:

- Proposing highly informative features, which allow training a simple classifier for state classification.
- Improving the reliability of fault detection through the application of statistical hypothesis testing.
- Showing the applicability of the proposed method on a low-power-consumption microcontroller.

The remainder of this paper is organized as follows: Sections II and III describe the power converters that are used in the experiments, and the considered feature types. In Section IV, a brief description of the classifier structure and training is given, while the cross-temporal integration method is introduced in Section V. Experiments are described in Section VI and their results are discussed in Section VII. The implementation of the proposed method on a low-power microcontroller is presented in Section VIII, before providing conclusions and an outlook on future work in Section IX.

II. POWER CONVERTER TOPOLOGIES

For the analysis, two converter topologies were selected, covering the most relevant challenges of modern power electronics. A frequently used and fundamental converter system is the step-down converter. A modular multilevel converter (MMC) consisting of three separate voltage-source converters with their typical non-constant DC-link voltage is chosen as a more complex and future-oriented test case.

The main components of the step-down converter are a DC-link capacitor, a self-commutated power electronic device and a diode. An inductor on the output side is used for smoothing the current, see Fig. 1. An insulated-gate bipolar transistor (IGBT) is used as a typical self-commutated power-electronic device. The IGBT is controlled by a digital control unit implementing a variable duty cycle d. A diode bridge connected to the mains voltage feeds the DC-link capacitor. On the output side, several resistors and inductors are

available. They are selected such that various states of operation are available. Certain states represent normal operation, while the other states emulate various degrees of degradation of components and are considered as fault states. The currents and voltages are heavily distorted due to the switching operation and present challenges for measurement and subsequent identification.

Since our proposed classification approach yielded extremely high precision on the step-down converter data, the MMC was selected as a more challenging system, cf. Fig. 1b. MMC converters are suggested for and, in a few cases, already used in modern static synchronous compensator systems (STATCOM). They improve power quality in transmission and distribution networks. Each sub-module consists of a four-quadrant converter with its own DC-link electrolytic capacitor. As typical for such STATCOM applications, they connect to the grid via a series inductor. A control unit stabilizes each DC-link and controls the magnitude of the current. MMC converters without proper control would become instable, consequently, the operating point for each of the three converters varies continuously—increasing the challenges for the identification of faults and aging. The modification of the DC capacitance is implemented by additional smaller capacitances that are added and removed. Modifications of the capacitance and modifications of the current magnitude both influence the variation observed in the DC-link voltage, making the separation of the two effects challenging. Regarding the specific case of capacitors, depending on the technology, different criteria have been accepted to asses the end-of-life. For the aluminum electrolytic capacitor, these are a capacitance reduction by 20% or an increase of the equivalent series resistance (ESR) by a factor of at least 2.5. For the multilayer ceramic capacitor, a capacitance reduction of 10% is regarded as a failure, while for the metalized polypropylene film capacitor, the failure threshold is at 5% [36].

III. FEATURE EXTRACTION

Appropriate features are important to speed the convergence and enhance the performance of machine-learning-based fault-diagnosis. Sometimes, using time-domain signals is sufficient, but in many other cases, e.g. when dealing with the degradation faults described in this paper, detecting the parameter changes directly from the time series is difficult.Deep learning techniques may help here, as they can learn optimal features during the training phase, but this approach is computationally expensive, typically requires larger amounts of representative and labeled data, and may not generalize well.

Therefore, in this work, one focus lies on developing appropriate signal processing for a feature extraction well-suited to subsequent deep learning. Two different signal processing techniques, WD and EMD, are used and compared for this purpose. As shown below, this allows for robust detection of parameter changes by using a low-complexity machine-learning-based classifier.

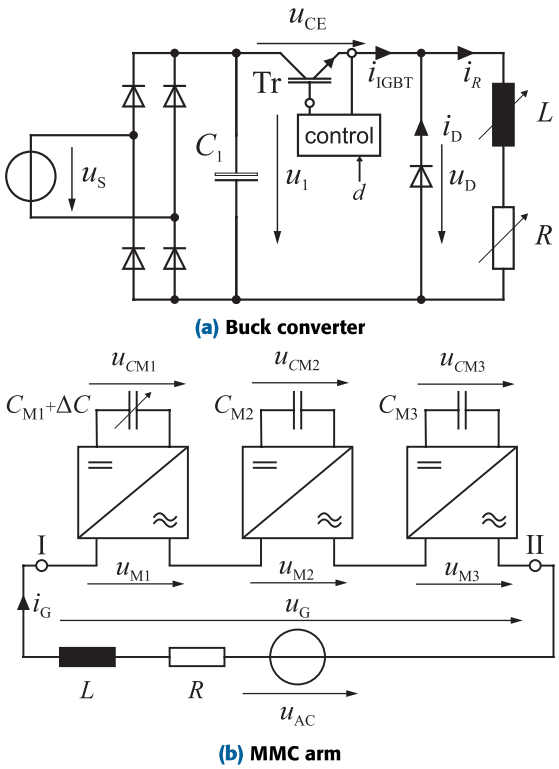

FIGURE 1. Considered power converter systems.

A. WAVELET DECOMPOSITION

The wavelet transform is one of the most popular techniques for the time-frequency analysis of non-stationary signals. It decomposes the signal into a selected number of components, where each component corresponds to a specific frequency range of the original signal. The process is called wavelet decomposition (WD); it can be achieved through the Mallat algorithm. For a given signal $X(t)$ with a frequency range from 0 to f_s, the first step in the WD is to filter the original signal with a pair of complementary high- and low-pass filters. The parameters of the filters are determined by the choice of wavelet function [37]. The component obtained at the output of the low-pass filter is called *approximation*; it corresponds to the frequency band $[0, f_s/2]$. Similarly, the second component, called *detail*, at the output of the high pass filter, corresponds to the frequency band $[f_s/2, f_s]$. After filtering, both components are down-sampled by a factor of two and the filtering procedure is repeated on the low-frequency components to generate a tree-like structure of coefficients. This yields a new approximation corresponding to the frequency band $[0, f_s/4]$ and a new detail corresponding to the frequency band $[f_s/4, f_s/2]$. Thus, if the decomposition is done on N levels, one approximation and N detail components will be extracted and the final approximation will correspond to the frequency band $[0, f_s/(2^N)]$.

B. EMPIRICAL MODE DECOMPOSITION

Empirical mode decomposition is a method for decomposing an input signal into a finite number of *intrinsic mode*

TABLE 1. Extracted statistical features.

Feature	Symbol
mean	μ
standard deviation	σ
variance	var
root mean square	RMS
skewness	SK
kurtosis	KU
crest factor	CF
shape factor	SF
mean absolute deviation	MAD
central moment	CM
range	RG
minimum	min
maximum	max

functions (IMFs). This is achieved through the *sifting* process [38] - an iterative algorithm that involves two steps: estimation of the upper envelope (UE) and lower envelope (LE), and data reduction. In the first step, the local maxima and minima of the signal are identified, and the UE and LE are constructed as cubic splines, connecting all local maxima and all local minima, respectively. The mean of the two envelopes is computed to obtain the so-called mean envelope. In the second step, the mean envelope is subtracted from the original signal to obtain a residual signal. The residual signal is then checked for the presence of an IMF. If an IMF is detected, it is extracted from the residual signal and added to the list of extracted IMFs. If no IMF is detected, the residual signal is considered as a trend and added to the final trend component. By definition, every IMF needs to satisfy two conditions. The first condition is that the number of extrema and the number of zero crossings in the whole length of the signal must either be equal or differ at most by one. The second condition is that, at any point, the mean value of the UE and LE is zero. Each extracted IMF represents one oscillation mode of the signal. After performing the EMD on the signal $X(t)$, the signal can be represented as:

$$X(t) = \sum_{n=1}^{N} c_n(t) + r_N(t), \tag{1}$$

where N is the number of the components, c_n is the n-th IMF and r_N is the residual, which represents a constant or a mean trend.

C. FEATURE EXTRACTION PROCEDURE

The top-level algorithm for feature extraction is the same for all types of features used in this paper. After selecting the appropriate signals for fault detection, features are extracted from each of these. The first step of feature extraction is always a windowing step, applying a selection window of fixed length to perform signal segmentation. Starting from the beginning of the signal, segments are obtained by successively moving a rectangular window by one quarter of its length. The part of the signal corresponding to the i-th segment is denoted as $\mathbf{X_i}$. The length of the selection window is always set to 2 seconds. The second step is that of actual feature extraction, which is carried out for each segment in all signals.

Two types of features are considered in this paper: The first type, the *energy-based features*, are always derived based on the WD. The main intuition for applying this feature choice comes from the fact that parameter changes in the system are reflected in the energy of the system voltages and currents [39]. As the components of a WD correspond to different frequency ranges, tracking the energy of each component allows more precise tracking of the signal changes overall. Different components are expected to be more sensitive to different types of changes, which makes them attractive features for FDI. This could not be achieved with standard frequency-based techniques such as *FFT* or *STFT*, since the soft faults produce a negligible change in the spectrum, outside of the signals base frequency.

Hence, after the segmentation of the signal, wavelet features are computed by first performing a WD for every $\mathbf{X_i}$ and then calculating the energy of each component of the WD. Finally, the energy of each component is divided by the sum of all energies of the extracted components. Using Daubechies wavelets this decomposition is conducted on 6 levels, yielding one approximation and 6 detail components, so the feature vector θ_i^{WDE} extracted from $\mathbf{X_i}$ has 7 components. This wavelet family provides a large flexibility in choosing the order of the filters and has shown good performance with fault detection applications [14], [16]. The second type of feature we consider are *statistical features*. These are computed either of the WD components or of the results of the EMD. The extraction procedure is very similar to the energy-based features. After the segmentation of the signal and a decomposition of each segment by means of either WD or EMD, a set of statistical parameters is computed for each extracted component of the decomposition. The list of all 13 computed statistical parameters is presented in Table 1. In the example of the 7-component WD, the feature vector θ_i^{WD} corresponding to frame $\mathbf{X_i}$ contains 13 statistical parameters for each of the 7 components, for a total of 91 dimensions. For the EMD, the first 8 IMFs are extracted, so the subsequent extraction of statistical parameters leads to a feature vector θ_i^{EMD} with 104 dimensions.

IV. CLASSIFICATION

We are proposing a new, interpretable and learning-based approach to detecting and classifying faults from time series signals, and we evaluate it on the described scenario of fault detection for power converter systems. The approach is built upon deep-neural-network (DNN) [40] based classifiers, which we integrate within a novel hybrid (neural/statistical) framework that combines the flexibility of deep learning with the interpretability and guarantees of statistical models. The constituent DNN component of the proposed system is a fully connected multi-layer model, trained as a classifier. The number of neurons in the input layer corresponds to the

dimension of the feature vector θ, while the number of the neurons in the output layer is equal to the number of possible classes K. The activation function of the neurons in all except for the output layer is a rectified linear unit, while for the output layer, a softmax activation function needs to be used in order to obtain outputs that are non-negative and normalized to sum to 1.

For training density estimators, we use the categorical cross-entropy as the loss function, hence the output of each neuron in the output layer corresponds to the estimated probability $p(k = i|\theta)$ of all converter states $i = 1 \ldots K$, given the feature vector. Training of this network was carried out using the Adam optimizer of the TensorFlow framework. Around 400 feature vectors were extracted from each state of the system. For training the classifier, 5-fold cross-validation was applied, with 80% of the data used in training and the remaining 20% in the evaluation in each of the 5 rounds, so that every data point ends up being used in training for 4 and in testing for 1 of the cross-validation runs.

V. SEQUENTIAL MULTI-HYPOTHESIS TESTING FOR DEEP-LEARNING MODELS

The performance of learning-based methods for FDI is highly dependent on the quality of the measurements. In the presence of noise or unexpected changes of the operating conditions, extracted features can become unreliable. For these reasons, even when plenty of data is available for training, it is almost impossible to obtain a classifier that will guarantee 100% accuracy. In practice, this can then lead to intermittent errors, like false alarms, causing unnecessary expense.

In order to arrive at a highly reliable decision process, our proposed, new framework embeds the deep-learning model into a hybrid, probabilistic architecture. It only commits to a classification decision after integrating the probability density information, which the DNN delivers, across time. This cross-temporal information integration is carried out by Bayesian sequential density estimation, and it is followed by a subsequent hypothesis test, which is achieved by applying an M-ary sequential probability ratio test (MSPRT) [41].

Given M possible hypotheses and the feature vectors for the last N time points, the MSPRT obtains the posterior probabilities for each of the possible hypotheses as

$$p(H_j|\theta_1, \theta_2, \ldots, \theta_N) = \frac{\pi_j \prod_{n=1}^{N} p(\theta_n|H_j)}{\sum_{k=0}^{M-1} \pi_k \prod_{n=1}^{N} p(\theta_n|H_k)}, \quad (2)$$

where π_j and $p(\theta_n|H_j)$ are the prior probability and the conditional probability of the current observation given hypothesis H_j, respectively. In our application, each hypothesis corresponds to one of the possible states of the system, while the observation likelihood $p(\theta_n|H_j)$ should be computed by the classifier. However, this is not immediately the case when the DNN is applied, since the neurons of the output layer instead give the posterior probability $p(H_j|\theta_n)$. Hence, a modification of Equation (2) is necessary, achieved by applying Bayes' rule:

$$\begin{aligned} p(H_j|\theta_1, \theta_2, \ldots, \theta_N) &= \frac{\pi_j \prod_{n=1}^{N} \frac{p(H_j|\theta_n)p(\theta_n)}{\pi_j}}{\sum_{k=0}^{K-1} \pi_k \prod_{n=1}^{N} \frac{p(H_k|\theta_n)p(\theta_n)}{\pi_k}} \\ &= \frac{\prod_{n=1}^{N} p(\theta_n) \prod_{n=1}^{N} p(H_j|\theta_n)}{\sum_{k=0}^{K-1} \prod_{n=1}^{N} p(\theta_n) \prod_{n=1}^{N} p(H_k|\theta_n)} \\ &= \frac{\prod_{n=1}^{N} p(H_j|\theta_n)}{\sum_{k=0}^{K-1} \prod_{n=1}^{N} p(H_k|\theta_n)} \end{aligned} \quad (3)$$

where $p(\theta_n)$ is the prior probability of the observation θ_n.

By the definition of the MSPRT, the decision for selecting a currently active hypothesis H_{active} is determined at the earliest time point N_c that fulfills the following conditions

$$\begin{aligned} N_c &= \text{first } N \geq 1 \text{ such that} \\ p(H_k|\theta_1, \theta_2, \ldots, \theta_N) &> \frac{1}{1 + A_k}, \quad \text{for some class } k \end{aligned} \quad (4)$$

where A_k defines the decision threshold for selecting hypothesis H_k as an active hypothesis. In general, this parameter should be chosen separately for each hypothesis and its values should always be positive and less than 1. In this way, the inequality $p(H_j|\theta_1, \theta_2, \ldots, \theta_N) > 1/(1 + A_j)$ can be fulfilled by at most one value of j. It should also be noted that for the case of two classes, the MSPRT is equivalent to Wald's test [42].

An important property of the MSPRT is that if $A_0 = A_1 = \ldots A_{M-1} = A$, the total probability ϵ of an incorrect decision is limited to

$$\epsilon \leq \frac{A}{1 + A}. \quad (5)$$

Based on this guarantee (which of course is predicated on the correctness of the underlying probability estimates), the value A can be selected depending on the desired upper bound of ϵ.

VI. EXPERIMENTS

For both selected converter types, the general procedure of experiments is the same. During the experiments, normal system conditions and fault conditions (with various degrees of difference) are set by a variation of selected system components. The selected set of voltages and currents is recorded continuously. To analyze the recordings, one or two most suitable signals—depending on the system under test—are used for the feature computation, which is performed in MATLAB. When all system parameters are at their nominal values, the system is considered to be in the normal state. When the value of one or more parameters is significantly changed, the system is considered to be in a fault state. Because the degradation of the parameters is, in general, a slow process, it was emulated by adding additional capacitance and inductance starting from very low modifications and ending with more noticeable changes.

A. DIAGNOSING BUCK CONVERTERS

A buck converter with the nominal parameters as given in Table 2 and the modifications of these parameters as given in Table 3 was set up (Fig. 1a).

With regard to practical applications, the variation of the load resistance does not mark fault states but is realistic irrespective of the system conditions, when typical, irregular, load changes occur during operation. A variation of capacitance or inductance, in contrast, is considered a fault. Voltages and currents were measured as given in Fig. 1a. As shown in Table 2, there are three nominal values of inductance. Hence, three variants of normal states were recorded, which only differ by the value of the nominal inductance. For each of these normal states, one or two additional components were added in order to change parameters for the emulation of faults. Combining the two values for additional capacitance and inductance, four different fault scenarios with one additional component were recorded for each of the nominal inductance values. Additionally, one scenario per normal state was recorded with two simultaneously added components (one additional capacitor and one additional inductor), leading to more pronounced parameter and behavioral deviations. During each experiment, the load resistance was irregularly changed between the four values given in Table 2 to represent extraneous load variations. For each experiment, the signals I_{IGBT}, I_R, U_D, and U_1 were recorded. The duration of each recording was set to 16 seconds; the duty cycle d was kept constant at 50 %, leading to worst-case current oscillation.

B. MMC EXPERIMENTS

For the MMC system shown in Fig. 1b, DC capacitance was varied to emulate the fault condition of capacitor degradation. It was realized by capacitors switched in parallel to the sub-module capacitors, implementing relative capacitance changes of 2%, 3%, 5%, or 7%. One set of the recordings covers the addition of capacitors to the capacitor C_{M1}. The same procedure was repeated when adding capacitors to the capacitor C_{M2}. For each of these scenarios, constant load and load variation were tested. In case of constant load operation, the effective arm current was kept constant. Load variation was emulated by an irregular variation of the effective arm current within the recording time interval. This variation of the current also affects the sub-module capacitor voltage, specifically by influencing the magnitude of its oscillation.

Consequently, load variation has a similar effect as increasing or decreasing the capacitance. Hence, these measurements test the robustness of the proposed FDI scheme, as discussed in Section VII. The duration of each recording is 120 seconds.

VII. RESULTS

One of the most important advantages of the proposed method is its ability to achieve a highly reliable detection of the system state through a combination of signal processing for feature extraction, deep learning for instantaneous probability estimation and an overall Bayesian decision-making, without the need for extensive recordings. In the following, we first analyze and compare performance of the approach with different feature sets. Finally, the effects of applying an MSPRT for final decision making are demonstrated.

TABLE 2. Nominal parameter values.

Parameter	Values
C	4 mF
L	5 mH, 10 mH, 20 mH
R	10 Ω, 14 Ω, 23 Ω, 34 Ω
d	50%

TABLE 3. Additional parameter values.

Component	Values
ΔL	160 μH, 800 μH
ΔC	47 μF, 540 μF

A. BUCK CONVERTER RESULTS

The output voltage signal was used for extracting features for FDI of the buck converter. WD-based energy features were employed for multi-class fault classification. The obtained results for the case when $L_nom = 20mH$ are shown in Table 4.

In all cases, a two-layer DNN with 15 neurons in the first and 10 neurons in the second layer is used for classification. The obtained accuracy is quite satisfactory. There are occasional errors between pairs of states with similar parameters, but they only occur in a few percent of the samples. This shows that the considered features are suitable to represent the characteristics of the different states of the system, letting a simple DNN structure obtain good initial classification results.

B. MMC RESULTS

In the case of the MMC, the arm current and the sub-module voltage output were used for feature extraction. Since the energy-based features did not show sufficient performance in preliminary experiments with this system, EMD- and WD-based statistical features were chosen instead. These features are extracted from the current and the voltage signal and then concatenated and fed into the DNN-based classifier. For both types of features, and in all tests in this subsection, the same DNN was used—a two-layer DNN, with 60 neurons in the first and 20 neurons in the second layer. To evaluate its capability of distinguishing all possible system states, first, a DNN was trained for multi-class classification of the normal and all fault states. As shown in the upper part of Table 5, when the arm current is constant, the classifier can make a clear distinction between different values of capacitance. Yet, it is also clear that the classifier cannot always separate the normal state and the state with the smallest capacitance change of 2%. The accuracy for each of these states is still above 90%, while for the other two cases, it is close to 100%.

TABLE 4. Confusion matrix for classification of buck converter states. Column annotations show the parameter change w.r.t. the nominal inductance/capacitance in %. Each cell shows the probability (in %) of recognizing the state denoted in the cell's column, when the true state is the one denoted in the corresponding row.

WD-based energy features						
	normal	ΔL=0.8	ΔL=4	ΔC=1	ΔC=12	ΔL=4, ΔC=12
Normal	98.1	0.0	1.9	0.0	0.0	0.0
$\Delta L = 0.8$	0.0	100.0	0.0	0.0	0.0	0.0
$\Delta L = 4$	1.8	0.0	98.2	0.0	0.0	0.0
$\Delta C = 1$	0.0	0.0	0.0	100.0	0.0	0.0
$\Delta C = 12$	0.0	0.0	0.0	0.00	95.8	4.2
$\Delta L = 4, \Delta C = 12$	0.0	0.0	0.0	0.0	0.0	100

TABLE 5. Confusion matrices for state classification of the MMC. Column annotations show the parameter change w.r.t. the nominal capacitance in %. Each cell shows the probability of recognizing the state denoted in the column, when the true state is denoted in the corresponding row.

Results for constant-current dataset				
WD-based statistical features				
	Normal	ΔC=2	ΔC=5	ΔC=7
Normal	99.2	0.8	0.0	0.0
$\Delta C = 2$	0.7	99.3	0.0	0.0
$\Delta C = 5$	0.0	0.0	97.1	2.9
$\Delta C = 7$	0.0	0.0	0.7	99.3
EMD-based statistical features				
	Normal	ΔC=2	ΔC=5	ΔC=7
Normal	96.1	2.6	1.3	0.0
$\Delta C = 2$	4.6	94.1	1.3	0.0
$\Delta C = 5$	0.0	0.8	97.9	1.3
$\Delta C = 7$	0.0	0.0	1.2	98.8
Results for dataset with changing current				
WD-based statistical features				
	Normal	ΔC=2	ΔC=5	ΔC=7
Normal	94.4	0.0	1.4	4.2
$\Delta C = 2$	1.2	98.8	0.0	0.0
$\Delta C = 5$	0.6	0.0	99.4	0.0
$\Delta C = 7$	3.1	0.0	4.7	92.2
EMD-based statistical features				
	Normal	ΔC=2	ΔC=5	ΔC=7
Normal	88.6	8.2	2.4	0.8
$\Delta C = 2$	2.0	91.7	4.9	1.4
$\Delta C = 5$	1.4	4.1	92.5	2.0
$\Delta C = 7$	2.1	1.4	8.6	87.9

The results for multi-class classification under changing load currents are shown in the lower part of Table 5.

As can be seen, both types of features are in principle appropriate for the task, but the WD-based features are clearly preferable. Understanding the exact reasons that allow for the better performance of WD-based features would require a more in-depth, theoretical study, which is outside the scope of this paper.

Since it is not possible to gather data that could reflect each possible change of capacitance, an important capability of data-based fault detection techniques is their potential for generalization. In order to assess this capability of the proposed approach, a DNN—with the same architecture as in the previous case—was trained as a binary classifier to recognize the difference between a normal and a fault state by using the data from normal operation and only representing fault states by data in which there is a capacitance change of exactly 2%. This classifier is then evaluated on data from those recordings, in which there is a 3%, 5%, and 7% change of capacitance. Results of this generalization experiment are shown in Table 6.

TABLE 6. Detecting changes of capacitance of the MMC above 2% w/ DNN trained to detect 2%. Column annotations show the parameter change w.r.t. nominal capacitance in %.

Results for constant-current dataset			
WD-based statistical features			
	ΔC=3	ΔC=5	ΔC=7
Accuracy[%]	98.2	98.0	99.1
EMD-based statistical features			
	ΔC=3	ΔC=5	ΔC=7
Accuracy[%]	95.0	95.1	97.3
Results for dataset with changing current			
WD-based statistical features			
	ΔC=3	ΔC=5	ΔC=7
Accuracy[%]	88.6	88.0	92.2
EMD-based statistical features			
	ΔC=3	ΔC=5	ΔC=7
Accuracy[%]	83.3	85.5	85.1

When the arm current is constant, and when WD-based statistical features are employed, the recognition rate is above 98% for all three fault states, which shows that there is a good separability between the normal and all of the fault conditions in the proposed feature space. For the data-set with the changing arm current, accuracy noticeably decreases, as shown in the lower part of Table 6. For the EMD based features the accuracy varies from 80% to 85%, whereas the WD-based features again show a better performance, with an accuracy around 90%. In the next subsection, we will show how these results can still be used as a basis for reliable detection. For this purpose, we will employ the proposed hybrid model, which allows for cross-temporal information integration on the basis of the learned DNN models.

C. HYBRID DIAGNOSTICS

For multi-class classification, the posterior probabilities of the system being in a certain state, as given at the output of the

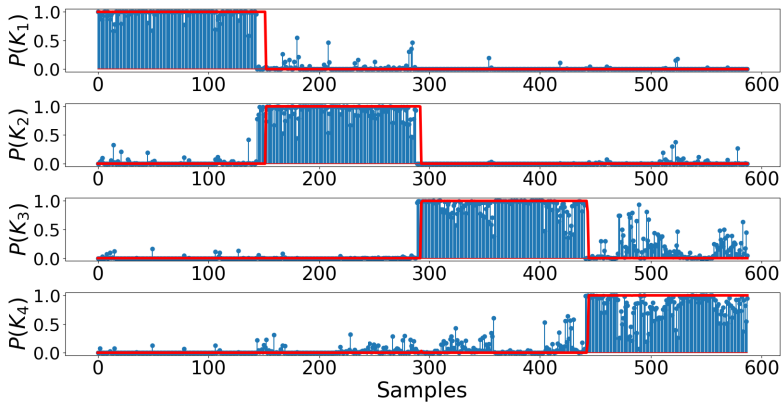

FIGURE 2. Posterior probabilities in multi-class classification for the dataset with changing currents, using EMD-based features, with (red) and w/o (blue) sequential hypothesis testing.

trained DNN, are used to compute the most probable system state with the help of the MSPRT. For these computations, we use 10 previous segments $\mathbf{X_i}$, which corresponds to the last 20 seconds of measurement data. The value of A in Equation (5) is chosen to be 0.001. This limits the maximal value of the total probability of an incorrect decision to $\epsilon \leq 0.01\%$, when assuming that the DNN yields correct probability estimates. The results for the test data were evaluated with a small grace period, onwards from 10 segments after there was a change in the state of the system.

Adopting this approach, the accuracy of fault detection improves to 100% for all test cases considered in Tables 4 and 5, so that fully reliable classification, error-free on all test data, is obtained with the suggested method.

Fig. 2 also illustrates this advantage in reliability, brought by the suggested use of an MSPRT, through a visualization of the class posterior probabilities without and with the cross-temporal information integration that the MSPRT affords. As can be seen, while the instantaneous likelihoods look rather noisy and contain many high values for those classes that may easily be confused with the given setup, the likelihoods after MSPRT are consistent across time, and tend to be either 1.0 in the correct class, or 0.0 for the incorrect class. The correctness of the MSPRT decisions is 100% in all considered cases, so that the likelihoods of 1.0 always indicate the correct class in our experiments, save for the lag time that we allow for changing system states.

Sequential hypothesis testing is then applied to the classifier that was trained only on changes of 2% and applied to mismatched cases of larger errors (3%, 5%, and 7%), for testing the robustness of the approach.

Using the MSPRT and following the above approach for evaluation, the classification accuracy is again improved to 100%, for all of the test cases shown in Table 6.

Although the precision of direct classification is below 90%, the decision of the MSPRT changes only after there is an actual change of the system state. The detection does come with a certain latency—however, for the detection of such small parameter changes, a latency in the order of seconds is not an issue.

VIII. ARDUINO IMPLEMENTATION

The developed FDI scheme was implemented and tested on the Arduino 33 BLE SENSE board. WD-based statistical features, as described in Section III, were employed; a pre-trained DNN was used for probability estimation and the sequential hypothesis testing on the last 10 samples was included as well. For implementing the WD, the library [43] was used. On the Arduino platform, a DNN framework is now available thanks to the TensorFlow Lite support for microcontrollers [44], which allows a two-step conversion from the standard TensorFlow model format to the one convenient for microcontrollers. Because of the quantization applied during the conversion process, a change of the performance of the model used for the Arduino application can be expected. To quantify this effect, the DNN used for obtaining the results in Table 5 with the wavelet-based statistical features was selected for a performance comparison. The segments of the signals used in the previous section were sent to the Arduino via USB serial interface, then the features were extracted and the fault probabilities were computed on the Arduino, after which new segments of data were sent. The final results obtained in this way are presented in Table 7.

As can be seen, there is a generally mild change in the instantaneous classification performance. For example, the detection accuracy of the normal state is reduced from 94.4% to 94.2%, and the capacitance change of 7% is now misclassified as the normal state with a higher likelihood of 5.1% rather than 3.1%. However, when hypothesis testing is applied, all results remain at 100%, so that the changes can be compensated fully through the proposed approach of cross-temporal integration.

Another measure of performance is the CPU time required, considering the feature extraction, DNN evaluation and hypothesis testing. In our tests, the average CPU time for one data segment of two seconds, measured on the Arduino, was about 500 *ms*. This comes as a consequence of the

TABLE 7. Confusion matrices for state classification of the MMC on the Arduino, compared with original results. Column annotations show the parameter change w.r.t. the nominal capacitance in %. Each cell shows the probability (in %) of recognizing the state denoted in the cell's column, when the true state is denoted in the row.

Results for dataset with changing current				
WD-based statistical features on the Arduino board				
	Normal	ΔC=2	ΔC=5	ΔC=7
Normal	94.2	0.0	1.4	4.4
ΔC = 2	1.7	98.3	0.0	0.0
ΔC = 5	0.6	0.0	99.4	0.0
ΔC = 7	5.1	0.1	5.2	89.6
WD-based statistical features - original results				
	Normal	ΔC=2	ΔC=5	ΔC=7
Normal	94.4	0.0	1.4	4.2
ΔC = 2	1.2	98.8	0.0	0.0
ΔC = 5	0.6	0.0	99.4	0.0
ΔC = 7	3.1	0.0	4.7	92.2

computation of a large number of statistical features for each signal, whereas DNN inference and hypothesis testing are not so time consuming. However, this does not have to be a drawback for the intended purpose of the described FDI scheme, which is to periodically check the current state of the system. As discussed in Sec. VII-C, the detection delay is always smaller than 10 segments, which corresponds to 20 seconds of recordings. Together with the computational time for each segment, the maximal detection delay is around 25 seconds. Thus, the proposed method is efficient enough to work on such a low-power device, which allows for a wide range of practical applications.

IX. CONCLUSION

This paper presents a novel condition-monitoring technique for parameter change detection in power converters. It relies on two types of signal-processing-based input features in conjunction with a hybrid classifier, consisting of a DNN-based posterior density estimator and a statistical model-based cross-temporal integration. The latter allows for controlling the total probability of classification errors.

Testing the proposed combination of features and classifier with data gathered in different scenarios for two types of power converters achieves high classification accuracy even with small parameter changes, and in different states of operation. The best performance was obtained using WD-based features. Additionally, it was shown that the approach can robustly detect changes that are unseen in the training phase. Additionally, the advantages of adding hypothesis testing on top of the classifier was shown for both systems. Finally, the computational efficiency and possible application of the proposed method is shown by providing a reference implementation on an Arduino 33 BLE SENSE board.

Future work will focus on applying the proposed method to other types of common faults occurring in power converters such as detecting and isolating OC faults using learning-based methods. Another challenge is developing an integrated fault detection system capable of monitoring a wide range of different faults, even of types unseen during training of the system. This case would call for an adaptation of the proposed approach to the domain of outlier detection, again, with the promise of high reliability due to the combined strengths of deep learning, cross-temporal information integration and subsequent hypothesis testing.

REFERENCES

[1] G. P. Adam, F. Alsokhiry, Y. Al-Turki, M. O. Ajangnay, and A. Y. Amogpai, "DC–DC converters for medium and high voltage applications," in *Proc. IECON 45th Annu. Conf. IEEE Ind. Electron. Soc.*, Oct. 2019, pp. 3337–3342.

[2] A. Lesnicar and R. Marquardt, "An innovative modular multilevel converter topology suitable for a wide power range," in *Proc. IEEE Bologna Power Tech. Conf.*, Jun. 2003, p. 6.

[3] S. Debnath, J. Qin, B. Bahrani, M. Saeedifard, and P. Barbosa, "Operation, control, and applications of the modular multilevel converter: A review," *IEEE Trans. Power Electron.*, vol. 30, no. 1, pp. 37–53, Jan. 2015.

[4] S. Yang, A. Bryant, P. Mawby, D. Xiang, L. Ran, and P. Tavner, "An industry-based survey of reliability in power electronic converters," in *Proc. IEEE Energy Convers. Congr. Expo.*, Sep. 2009, pp. 3151–3157.

[5] Z. Zhao, K. Li, Y. Jiang, S. Lu, and L. Yuan, "Overview on reliability of modular multilevel cascade converters," *Chin. J. Elect. Eng.*, vol. 1, no. 1, pp. 37–49, Dec. 2015.

[6] S. Yang, A. Bryant, P. Mawby, D. Xiang, L. Ran, and P. Tavner, "An industry-based survey of reliability in power electronic converters," *IEEE Trans. Ind. Appl.*, vol. 47, no. 3, pp. 1441–1451, May/Jun. 2011.

[7] S. Nie, X. Pei, Y. Chen, and Y. Kang, "Fault diagnosis of PWM DC–DC converters based on magnetic component voltages equation," *IEEE Trans. Power Electron.*, vol. 29, no. 9, pp. 4978–4988, Sep. 2014.

[8] H. Givi, E. Farjah, and T. Ghanbari, "Switch and diode fault diagnosis in nonisolated DC–DC converters using diode voltage signature," *IEEE Trans. Ind. Electron.*, vol. 65, no. 2, pp. 1606–1615, Feb. 2018.

[9] S. S. Khan and H. Wen, "A comprehensive review of fault diagnosis and tolerant control in DC–DC converters for DC microgrids," *IEEE Access*, vol. 9, pp. 80100–80127, 2021.

[10] H. Gara and K. Ben Saad, "Fault detection for linear switched systems based on a bank of Luenberger observers," in *Proc. Int. Conf. Adv. Syst. Electric Technol. (IC_ASET)*, Mar. 2018, pp. 92–97.

[11] J. Poon, P. Jain, I. C. Konstantakopoulos, C. Spanos, S. K. Panda, and S. R. Sander, "Model-based fault detection and identification for switching power converters," *IEEE Trans. Power Electron.*, vol. 32, no. 2, pp. 1419–1430, Feb. 2016.

[12] Z. Cen and P. Stewart, "Condition parameter estimation for photovoltaic buck converters based on adaptive model observers," *IEEE Trans. Rel.*, vol. 66, no. 1, pp. 148–160, Mar. 2017.

[13] Y. Jiang, Y. Yu, and X. Peng, "Online anomaly detection in DC/DC converters by statistical feature estimation using GPR and GA," *IEEE Trans. Power Electron.*, vol. 35, no. 10, pp. 10945–10957, Oct. 2020.

[14] Q. Sun, Y. Wang, and Y. Jiang, "A novel fault diagnostic approach for DC–DC converters based on CSA-DBN," *IEEE Access*, vol. 6, pp. 6273–6285, 2018.

[15] L. Wang, F. Lyu, Y. Su, and J. Yue, "Kernel entropy-based classification approach for superbuck converter circuit fault diagnosis," *IEEE Access*, vol. 6, pp. 45504–45514, 2018.

[16] N. Markovic, T. Stoetzel, V. Staudt, and D. Kolossa, "Hybrid condition monitoring for power electronic systems," in *Proc. 18th IEEE Int. Conf. Mach. Learn. Appl. (ICMLA)*, Dec. 2019, pp. 1687–1694.

[17] S. Zhao, F. Blaabjerg, and H. Wang, "An overview of artificial intelligence applications for power electronics," *IEEE Trans. Power Electron.*, vol. 36, no. 4, pp. 4633–4658, Apr. 2021.

[18] D. Ronanki and S. S. Williamson, "Failure prediction of submodule capacitors in modular multilevel converter by monitoring the intrinsic capacitor voltage fluctuations," *IEEE Trans. Ind. Electron.*, vol. 67, no. 4, pp. 2585–2594, Apr. 2020.

[19] M. Asoodar, M. Nahalparvari, C. Danielsson, R. Soderstrom, and H.-P. Nee, "Online health monitoring of DC-link capacitors in modular multilevel converters for FACTS and HVDC applications," *IEEE Trans. Power Electron.*, vol. 36, no. 12, pp. 13489–13503, Dec. 2021.

[20] Z. Wang and L. Peng, "Grouping capacitor voltage estimation and fault diagnosis with capacitance self-updating in modular multilevel converters," *IEEE Trans. Power Electron.*, vol. 36, no. 2, pp. 1532–1543, Feb. 2021.
[21] K. Wang, L. Jin, G. Li, Y. Deng, and X. He, "Online capacitance estimation of submodule capacitors for modular multilevel converter with nearest level modulation," *IEEE Trans. Power Electron.*, vol. 35, no. 7, pp. 6678–6681, Jul. 2020.
[22] C. Liu, F. Deng, Q. Yu, Y. Wang, F. Blaabjerg, and X. Cai, "Submodule capacitance monitoring strategy for phase-shifted carrier pulsewidth-modulation-based modular multilevel converters," *IEEE Trans. Ind. Electron.*, vol. 68, no. 9, pp. 8753–8767, Sep. 2021.
[23] Q. Pu, L. Qin, Q. Wang, J. Le, and K. Liu, "Online monitoring and balancing for MMC capacitor aging," in *Proc. 4th IEEE Workshop Electron. Grid (eGRID)*, Nov. 2019, pp. 1–6.
[24] J. Hu, G. Qiu, W. Wang, L. Ran, K. Ma, and H. Jiang, "An on-line capacitor condition monitoring method based on switching frequencies for modular multilevel converters," in *Proc. 4th Int. Conf. Energy, Electr. Power Eng. (CEEPE)*, Apr. 2021, pp. 183–187.
[25] Z. Geng, M. Han, and G. Zhou, "Switching signals based condition monitoring for submodule capacitors in modular multilevel converters," *IEEE Trans. Circuits Syst. II, Exp. Briefs*, vol. 68, no. 6, pp. 2017–2021, Jun. 2021.
[26] Z. Wang, Y. Zhang, H. Wang, and F. Blaabjerg, "A reference submodule based capacitor condition monitoring method for modular multilevel converters," *IEEE Trans. Power Electron.*, vol. 35, no. 7, pp. 6691–6696, Jul. 2020.
[27] H. Wang, H. Wang, Z. Wang, Y. Zhang, X. Pei, and Y. Kang, "Condition monitoring for submodule capacitors in modular multilevel converters," *IEEE Trans. Power Electron.*, vol. 34, no. 11, pp. 10403–10407, Nov. 2019.
[28] N. Markovic, D. Vahle, V. Staudt, and D. Kolossa, "Condition monitoring for power converters via deep one-class classification," in *Proc. 20th IEEE Int. Conf. Mach. Learn. Appl. (ICMLA)*, Dec. 2021, pp. 1513–1520.
[29] W. Chen and A. M. Bazzi, "Logic-based methods for intelligent fault diagnosis and recovery in power electronics," *IEEE Trans. Power Electron.*, vol. 32, no. 7, pp. 5573–5589, Jul. 2017.
[30] M. Houchati, L. Ben-Brahim, A. Gastli, and N. Meskin, "Fault detection in modular multilevel converter using principle component analysis," in *Proc. IEEE 12th Int. Conf. Compat., Power Electron. Power Eng. (CPE-POWERENG)*, Apr. 2018, pp. 1–6.
[31] H. Yang, W. Zhou, J. Sheng, H. Luo, C. Li, W. Li, and X. He, "A statistical submodule open-circuit failure diagnosis method for modular multilevel converters (MMCs) with variance measurement," *IEEE Open J. Power Electron.*, vol. 1, pp. 180–189, 2020.
[32] B. Cai, Y. Zhao, H. Liu, and M. Xie, "A data-driven fault diagnosis methodology in three-phase inverters for PMSM drive systems," *IEEE Trans. Power Electron.*, vol. 32, no. 7, pp. 5590–5600, Jul. 2017.
[33] F. Deng, M. Jin, C. Liu, M. Liserre, and W. Chen, "Switch open-circuit fault localization strategy for MMCs using sliding-time window based features extraction algorithm," *IEEE Trans. Ind. Electron.*, vol. 68, no. 10, pp. 10193–10206, Oct. 2021.
[34] S.-H. Kim, D.-Y. Yoo, S.-W. An, Y.-S. Park, J.-W. Lee, and K.-B. Lee, "Fault detection method using a convolution neural network for hybrid active neutral-point clamped inverters," *IEEE Access*, vol. 8, pp. 140632–140642, 2020.
[35] S. Kiranyaz, A. Gastli, L. Ben-Brahim, N. Al-Emadi, and M. Gabbouj, "Real-time fault detection and identification for MMC using 1-D convolutional neural networks," *IEEE Trans. Ind. Electron.*, vol. 66, no. 11, pp. 8760–8771, Nov. 2019.
[36] H. Wang and F. Blaabjerg, "Reliability of capacitors for DC-link applications in power electronic converters—An overview," *IEEE Trans. Ind. Appl.*, vol. 50, no. 5, pp. 3569–3578, Sep. 2014.
[37] S. G. Mallat, "A theory for multiresolution signal decomposition: The wavelet representation," *IEEE Trans. Pattern Anal. Mach. Intell.*, vol. 11, no. 7, pp. 674–693, Jul. 1989.
[38] N. E. Huang, "The empirical mode decomposition and the Hilbert spectrum for nonlinear and non-stationary time series analysis," *Proc. Roy. Soc. London Ser. A, Math., Phys. Eng. Sci.*, vol. 454, no. 1971, pp. 903–995, Mar. 1998.
[39] C. Wu, J. Yue, L. Wang, and F. Lyu, "Detection and classification of recessive weakness in superbuck converter based on WPD-PCA and probabilistic neural network," *Electronics*, vol. 8, no. 3, p. 290, Mar. 2019.
[40] K. Gurney, *An Introduction to Neural Networks*. New York, NY, USA: Taylor & Francis e-Library, 2004.
[41] C. W. Baum and V. V. Veeravalli, "A sequential procedure for multihypothesis testing," *IEEE Trans. Inf. Theory*, vol. 40, no. 6, pp. 1994–2007, Nov. 1994.
[42] A. Wald, "Sequential tests of statistical hypotheses," *Ann. Math. Statist.*, vol. 16, no. 2, pp. 117–186, Jun. 1945.
[43] R. Hussain, *Wavelib*. San Francisco, CA, USA: GitHub Repository, 2019.
[44] P. Warden and D. Situnayake, *TinyML: Machine Learning With TensorFlow Lite on Arduino and Ultra-Low-Power Microcontrollers*, 1st ed. Springfield, MO, USA: O'Reilly, 2019.

NIKOLA MARKOVIC (Graduate Student Member, IEEE) was born in Jagodina, Serbia. He received the B.Sc. and M.Sc. degrees in electrical engineering from the University of Belgrade, Serbia, in 2015 and 2016, respectively. He is currently pursuing the Ph.D. degree with Technische Universität Berlin.

From 2016 to 2018, he was with the Institute Mihajlo Pupin as a Research and Development Engineer. In 2016, he did a three-month internship with the Statistical Artificial Intelligence Laboratory, Ulsan National Institute of Technology. From 2018 to 2022, he was a Research Assistant with Ruhr University Bochum.

THOMAS STOETZEL (Student Member, IEEE) was born in Dortmund, Germany. He received the B.Sc. and M.Sc. degrees in electrical engineering and information technology from Ruhr University Bochum, Germany, in 2013 and 2015, respectively, where he is currently pursuing the Ph.D. degree. He has been with the Institute of Power Systems Technology and Power Mechatronics, Ruhr University Bochum, as a Research Assistant, since 2016. His research interest includes the application of power-electronic converters in grid-connected applications, with a focus on high-voltage DC transmission systems (HVDC), including the monitoring of such systems during operation.

VOLKER STAUDT (Senior Member, IEEE) received the Dipl.-Ing. and Dr.-Ing. degrees in electrical engineering from Ruhr University Bochum, Germany, in 1987 and 1993, respectively. He has been a Professor with the Institute of Power Systems Technology and Power Mechatronics, Ruhr University Bochum, since 2009. His research interests include power electronic converters connected to the grid, converter-fed machines, power theory, compensation strategies, and signal analysis in the scope of electrical power engineering.

DOROTHEA KOLOSSA (Senior Member, IEEE) was born in Paderborn, Germany. She received the Dipl.-Ing. degree in computer engineering and the Dr.-Ing. degree in electrical engineering from Technische Universität Berlin (TU Berlin), Germany, in 1999 and 2007, respectively.

She was a Research Assistant in control systems design with the DaimlerChrysler Research and Technology, Hennigsdorf, TU Berlin, and a Visiting Faculty with Parlab, UC Berkeley, before joining Ruhr-Universität Bochum, Germany, in 2010, where she was a Faculty Member of the Institute of Communication Acoustics, until 2022. In October 2022, she joined TU Berlin as a Professor with the Institute of Energy and Automation Technology. She has published almost 200 peer-reviewed journal articles and conference papers, and book chapters.

Prof. Kolossa is an Associate Member of the IEEE Audio and Acoustic Signal Processing Technical Committee and a Council Member of the EAA TC on Audio Signal Processing.